Synthesis, Electrochemical Behavior, and Spectroscopic and Luminescence Properties of Dinuclear Species Containing $[Ru(diimine)_3]^{2+}$ and $[Re(diimine)Cl(CO)_3]$ Chromophores Bridged by a Nonsymmetric Quaterpyridine Ligand

David A. Bardwell,[†] Francesco Barigelletti,*[,‡] Rosemary L. Cleary,[†] Lucia Flamigni,[‡] Massimo Guardigli,[‡] John C. Jeffery,[†] and Michael D. Ward*[,†]

School of Chemistry, University of Bristol, Cantock's Close, Bristol BS8 1TS, U.K., and Istituto FRAE-CNR, Via P. Gobetti 101, 40129 Bologna, Italy

Received December 6, 1994[⊗]

The syntheses, electrochemical properties, ground state absorption spectra, luminescence spectra, and lifetimes of a series of homo- and heterodinuclear (and related mononuclear) complexes, containing a dicationic $[Ru(bpy)_3]^{2+}$-type chromophore (bpy = 2,2′-bipyridine) and/or a neutral $[ReCl(CO)_3(bpy)]$-type chromophore, are described. The connecting ligand is the asymmetric 2,2′:3′,2″:6″,2‴-quaterpyridine, L, which contains two inequivalent bipyridyl binding sites **A** and **B**, of which the "internal" site (**B**) is more sterically hindered than the "external" site (**A**). The X-ray structure of $[(CO)_3ClReLRu(bpy)_2][PF_6]_2 \cdot 2MeCN \cdot 0.5Et_2O$ (**Re^{I}-AB-Ru^{II}**) has been determined: $C_{49}H_{41}ClF_{12}N_{10}O_{3.5}P_2ReRu$, triclinic, $P\bar{1}$; $a = 10.449(7)$ Å, $b = 12.493(8)$ Å, $c = 22.906(11)$ Å, $\alpha = 92.83(5)°$, $\beta = 101.11(5)°$, $\gamma = 109.30(5)°$, $Z = 2$; 9685 independent data ($4° \leq 2\theta \leq 50°$) were refined on F^2 to final residuals of $wR_2 = 0.129$ ($R_1 = 0.046$). The Re(I) fragment is coordinated to the A site of L and the Ru(II) fragment is coordinated to the B site; the two bipyridine moieties of L are nearly perpendicular (86°) to minimize the steric interaction between the halves of the complex, and whereas the $\{Re(CO)_3Cl\}$ fragment coordinated to the A site has typical structural parameters, the $\{Ru(bpy)_2\}^{2+}$ fragment at the more sterically hindered B site displays noticeable lengthening of one of the Ru−N bonds. From a comparison of the electrochemical and spectroscopic properties of the complexes, it is found that when one chromophore occupies the A site (i) it is easier to oxidize and (ii) its lowest-lying metal-to-ligand charge-transfer excited state lies at lower energy, than when the same chromophore is linked to the B site. Thus, for **Ru^{II}-AB-Re^{I}** the luminescent state is centered on the Ru-based moiety, while for the positional isomer $[(CO)_3ClReLRu(bpy)_2]^{2+}$ (**Re^{I}-AB-Ru^{II}**) the luminescence is Re-centered. Thus intercomponent energy transfer (Dexter mechanism) takes place from a higher-lying Re-based level to the lowest-lying Ru-based luminescent level in **Ru^{II}-AB-Re^{I}** and a reversed Ru → Re energy transfer operates in **Re^{I}-AB-Ru^{II}**.

Introduction

The study of photoinduced electron transfer and energy transfer between components of "supramolecular" entities is of fundamental importance for the design of nanoscale devices capable of performing useful light-induced functions.[1] Polynuclear complexes containing different luminescent centers are of special interest, since intercomponent processes can be investigated by monitoring the emission properties.[2−5] For instance, in the presence of favorable spectroscopic properties of the metal-based fragments, emission can occur from one center after selective irradiation of the other center. In this way one may obtain information concerning the efficiency of the intramolecular energy-transfer process as a function of geometrical and structural parameters such as the metal−metal separation and the nature of the bridging ligand.

The low-spin d^6 metal complexes $[Ru(bpy)_3]^{2+}$,[6] $[Os(bpy)_3]^{2+}$,[7] and $[Re(bpy)(CO)_3Cl]^{8-10}$ (bpy = 2,2′-bipyridine) and related complexes are extensively employed as components of polynuclear systems because of their favorable excited-state and redox properties; in addition, these properties may be conveniently modified by adding peripheral substituents to the ligands. Thus, much recent work has focused on Ru(II)/Os(II) polypyridine systems in which excitation of the Ru(II) center results in emission from the metal-to-ligand charge-transfer (MLCT) excited state of the Os(II) center following intercomponent energy transfer, in some cases over long distances.[4] Re(I)/Ru(II) systems have been studied rather less although they show similar behavior, with irradiation of the Re(I) center

[†] University of Bristol.
[‡] Istituto FRAE-CNR.
[⊗] Abstract published in *Advance ACS Abstracts,* April 1, 1995.

(1) Balzani, V.; Scandola, F. *Supramolecular Photochemistry;* Ellis Horwood: Chichester, U.K., 1991.
(2) For a comprehensive review see ref 3. Some recent work is quoted in refs 4 and 5.
(3) Scandola, F.; Indelli, M. T.; Chiorboli, C.; Bignozzi, C. A. *Top. Curr. Chem.* **1990**, *158*, 73.
(4) (a) De Cola, L.; Balzani, V.; Barigelletti, F.; Flamigni, L.; Belser, P.; von Zelewsky, A.; Frank, M.; Vögtle, F. *Inorg. Chem.* **1993**, *32*, 5228. (b) Vögtle, F.; Frank, M.; Nieger, M.; Belser, P.; von Zelewsky, A.; Balzani, V.; Barigelletti, F.; De Cola, L.; Flamigni, L. *Angew. Chem., Int. Ed. Engl.* **1993**, *32*, 1643. (c) Barigelletti, F.; Flamigni, L.; Balzani, V.; Collin, J.-P.; Sauvage, J.-P.; Sour, A.; Constable, E. C.; Cargill Thompson, A. M. W. *J. Chem. Soc., Chem. Commun.* **1993**, 942. (d) Belser, P.; von Zelewsky, A.; Frank, M.; Seel, C.; Vögtle, F.; De Cola, L.; Barigelletti, F.; Balzani, V. *J. Am. Chem. Soc.* **1993**, *115*, 4076. (e) Giuffrida, G.; Calogero, G.; Guglielmo, G.; Ricevuto, V.; Ciano, M.; Campagna, S. *Inorg. Chem.* **1993**, *32*, 1179. (f) Richter, M. M.; Brewer, K. J. *Inorg. Chem.* **1992**, *31*, 1594. (g) Serroni, S.; Denti, G. *Inorg. Chem.* **1992**, *31*, 4251. (h) Denti, G.; Campagna, S.; Serroni, S.; Ciano, M.; Balzani, V. *J. Am. Chem. Soc.* **1992**, *114*, 2944. (i) Thummel, R. P.; Williamson, D.; Hery, C. *Inorg. Chem.* **1993**, *32*, 1587. (j) Arana, C.; Abruña, H. *Inorg. Chem.* **1993**, *32*, 194. (k) Furue, M.; Yoshidzumi, T.; Kinoshita, S.; Kushida, T.; Nozakura, S.; Kamachi, M. *Bull. Chem. Soc. Jpn.* **1991**, *64*, 1632. (l) Denti, G.; Serroni, S.; Camapagna, S.; Ricevuto, V.; Balzani, V. *Coord. Chem. Rev.* **1991**, *111*, 227. (m) Furue, M.; Maruyama, K.; Kanematsu, Y.; Kushida, T.; Kamachi, M. *Coord. Chem. Rev.* **1994**, *132*, 201. (n) Bignozzi, C. A.; Argazzi, R.; Chiorboli, C.; Scandola, F.; Dyer, R. B.; Schoonover, J. R.; Meyer, T. J. *Inorg. Chem.* **1994**, *33*, 1652. (o) Juris, A.; Balzani, V.; Campagna, S.; Denti, G.; Serroni, S.; Frei, G.; Güdel, H. U. *Inorg. Chem.* **1994**, *33*, 1491.

0020-1669/95/1334-2438$09.00/0

Chart 1

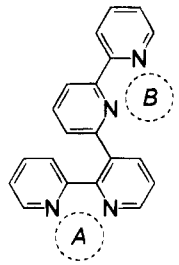

2,2':3',2":6",2"'-quaterpyridine

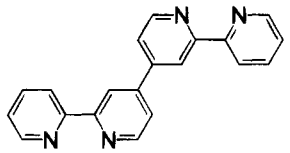

2,2':4',4":2",2"'-quaterpyridine

resulting in energy transfer to, and subsequent emission from, the Ru(II) center.[5] Energy transfer in the Re(I)/Ru(II) systems studied so far always proceeds in this direction since a Ru(II)-based MLCT excited state is typically lower in energy than a Re(I)-based MLCT excited state.

In this paper, we describe the syntheses and the electrochemical, spectroscopic, and photophysical properties of a series of Ru(II), Re(I), and mixed Ru(II)/Re(I) complexes of the nonsymmetric dinucleating ligand 2,2': 3',2":6",2"'-quaterpyridine (L = **AB**), which contains two inequivalent bpy-type chelating sites of which one is more sterically hindered than the other[11] (Chart 1 shows L with the related symmetric ligand 2,2':4',4": 2",2"' quaterpyridine[12]).

The inequivalent **A** and **B** sites are expected to affect to a different extent the MLCT energy levels of the attached chromophores, and this may allow modulation of the directionality of energy transfer between them. In fact, the following are important features of this bridging ligand: (i) the precise electrochemical, photophysical and spectroscopic properties of coordinated metal fragments will be site-specific due to the asymmetry of the ligand; (ii) the metal centers in dinuclear complexes will be sufficiently close, resulting in a significant ground-state electronic interaction between them; and (iii) there is the possibility of positional isomers in heterodinuclear complexes.

The complexes described in this paper are $[(bpy)_2RuL][PF_6]_2$ (**Ru^{II}-AB**), $[(bpy)_2RuLRu(bpy)_2][PF_6]_4$ (**Ru^{II}-AB-Ru^{II}**), $[(CO)_3ClReL]$ (**Re^{I}-AB**), $[(CO)_3ClReLReCl(CO)_3]$ (**Re^{I}-AB-Re^{I}**), $[(bpy)_2RuLReCl(CO)_3][PF_6]_2$ (**Ru^{II}-AB-Re^{I}**), and $[(CO)_3ClReLRu(bpy)_2][PF_6]_2$ (**Re^{I}-AB-Ru^{II}**). In all cases the first metal in the formula is coordinated at the "external", less hindered binding site (labeled **A**); the second metal in the formulas of the dinuclear complexes is coordinated at the "internal", more hindered binding site (labeled **B**). The inequivalence of the two bipyridyl binding sites has a considerable effect on the photophysical properties of the isomeric pair of complexes **Ru^{II}-AB-Re^{I}** and **Re^{I}-AB-Ru^{II}**, of which the latter has been crystallographically characterized.

Experimental Section

Materials and Synthetic Procedures. Organic starting materials were purchased from Aldrich and used as received; $[Re(CO)_5Cl]$ and $RuCl_3 \cdot xH_2O$ were obtained from Johnson Matthey. The ligand L,[11a] complexes **Ru^{II}-AB** and **Ru^{II}-AB-Ru^{II}**,[11a] and $[Ru(bpy)_2Cl_2]\cdot 2H_2O$[13] were prepared according to the published methods.

$[(CO)_3ClReL]$ (Re^{I}-AB). A mixture of $[Re(CO)_5Cl]$ (0.1 g, 0.28 mmol) and L (0.096 g, 0.31 mmol) was heated to reflux in toluene (30 cm^3) for 1 h to give a yellow suspension. After cooling to room temperature, followed by overnight refrigeration, the product was collected by filtration and air-dried. Yield: 70%.

$[(CO)_3ClReLReCl(CO)_3]$ (Re^{I}-AB-Re^{I}). A mixture of $[Re(CO)_5Cl]$ (0.25 g, 0.7 mmol) and L (0.10 g, 0.32 mmol) was heated to reflux in toluene (20 cm^3) for 24 h to give a yellow suspension. After cooling to room temperature, followed by overnight refrigeration, the product was collected by filtration, washed with CH_2Cl_2, and air-dried. Yield: 67%.

$[(bpy)_2RuLReCl(CO)_3][PF_6]_2$ (Ru^{II}-AB-Re^{I}). A mixture of **Ru^{II}-AB** (0.10 g, 0.1 mmol) and $[Re(CO)_5Cl]$ (0.073 g, 0.2 mmol) was heated to reflux in MeCN (20 cm^3) under N_2 for 18 h to give a dark orange/red solution. After cooling, the solvent was removed *in vacuo* and the crude reaction mixture purified by preparative-scale thin-layer chromatography on a 1.5 mm thick alumina plate (Merck article 5726) with MeCN/toluene (2:1, v/v) as eluent. The major orange/red band was scraped off and the product dissolved off it into MeCN. After concentration *in vacuo*, addition of ether precipitated the product as a red microcrystalline solid, which was collected by filtration and air-dried. Yield: 90%.

$[(CO)_3ClReLRu(bpy)_2][PF_6]_2$ (Re^{I}-AB-Ru^{II}). A mixture of **Re^{I}-AB** (0.10 g, 0.16 mmol) and $[Ru(bpy)_2Cl_2]\cdot 2H_2O$ (0.085 g, 0.16 mmol) was heated to 160 °C in ethylene glycol for 2 h to give an orange/red solution. After this solution was cooled to room temperature, excess aqueous NH_4PF_6 was added to precipitate the complex. The suspension was extracted with several portions of CH_2Cl_2; the combined extracts were dried ($MgSO_4$) and evaporated to dryness. The crude product was purified by chromatography on an alumina plate with MeCN/toluene (2:1, v/v) as above followed by recrystallization from MeCN/Et_2O to give X-ray-quality orange needles. Yield: 89%.

Analytical and spectroscopic data for the new complexes are summarized in Table 1.

Crystal Structure Determination of $[(CO)_3ClReLRu(bpy)_2][PF_6]_2 \cdot 2MeCN \cdot 0.5Et_2O$. Orange needles suitable for X-ray diffraction were grown from acetonitrile/ether by vapor diffusion. A suitable crystal (0.7 × 0.2 × 0.2 mm) was mounted in a capillary tube filled with mother liquor to prevent loss of solvent of crystallization. Crystallographic data are summarized in Table 2. Intensity data were collected using a Siemens R3m/V four-circle diffractometer (293 K, Mo Kα X-radiation, graphite monochromator, $\bar{\lambda} = 0.710\,73$ Å) in the range $4° \le 2\theta \le 50°$ by the Wyckoff ω-scan technique with index ranges $0 \le h \le 12$, $-14 \le k \le 14$, $-27 \le l \le 26$. A total of 10 261 reflections were collected, of which 9685 were unique ($R_{int} = 0.0233$). The data were corrected for Lorentz, polarization, and X-ray absorption effects,

(5) (a) Furue, M.; Naiki, M.; Kanematsu, Y.; Kushida, T.; Kamachi, M.; *Coord. Chem. Rev.* **1991**, *111*, 221. (b) van Wallendael, S.; Perkovic, M. W.; Rillema, D. P.; *Inorg. Chim. Acta* **1993**, *213*, 253. (c) Argazzi, R.; Bignozzi, C. A.; Bortolini, O.; Traldi, P. *Inorg. Chem.* **1993**, *32*, 1222. (d) Schoonover, J. R.; Gordon, K. C.; Argazzi, R.; Woodruff, W. H.; Peterson, K. A.; Bignozzi, C. A.; Dyer, R. B.; Meyer, T. J. *J. Am. Chem. Soc.* **1993**, *115*, 10996.

(6) (a) Meyer, T. J. *Pure Appl. Chem.* **1986**, *58*, 1193. (b) Juris, A.; Balzani, V.; Barigelletti, F.; Campagna, S.; Belser, P.; von Zelewsky, A. *Coord. Chem. Rev.* **1988**, *84*, 85. (c) Kalyanasundaram, K. *Coord. Chem. Rev.* **1982**, *46*, 159.

(7) (a) Kober, E. M.; Caspar, J. V.; Sullivan, B. P.; Meyer, T. J. *Inorg. Chem.* **1988**, *27*, 4587. (b) Brewer, R. G.; Jensen, G. E.; Brewer, K. J. *Inorg. Chem.* **1994**, *33*, 124.

(8) (a) Schanze, S. K; MacQueen, D. B.; Perkins, T. A.; Cabana, L. A. *Coord. Chem. Rev.* **1993**, *122*, 63. (b) Thornton, N. B.; Schanze, K. S. *Inorg. Chem.* **1993**, *32*, 4994. (c) Wang, Y.; Hauser, B. T.; Rooney, M. M.; Burton, R. D.; Schanze, K. S. *J. Am. Chem. Soc.* **1993**, *115*, 5675. (d) Spellane, P.; Watts, R. J.; Vogler, A. *Inorg. Chem.* **1993**, *32*, 5633. (e) Kotch, T. G.; Lees, A. J.; Fuerniss, S. J.; Papathomas, K. I.; Snyder, R.W. *Inorg. Chem.* **1993**, *32*, 2570. (f) Lee, Y. F.; Kirchhoff, J. R. *J. Am. Chem Soc.* **1994**, *116*, 3599. (g) Zipp, A. P.; Sacksteder, L.; Streich, J.; Cook, A. Demas, J. N.; DeGraff, B. A. *Inorg. Chem.* **1993**, *32*, 5629.

(9) (a) Worl, L. A.; Duesing, R.; Chen, P.; Della Ciana, L.; Meyer, T. J. *J. Chem. Soc., Dalton Trans.* **1991**, 849. (b) Wang, Y.; Schanze, K. S. *Inorg. Chem.* **1994**, *33*, 1354.

(10) (a) Juris, A.; Campagna, S.; Bidd, I.; Lehn, J.-M.; Ziessel, R. *Inorg. Chem.* **1988**, *27*, 4007. (b) Wallace, L.; Rillema, P. *Inorg. Chem.* **1993**, *32*, 3843. (c) Sacksteder, L.; Lee, M.; Demas, J. N.; DeGraff, B. A. *J. Am. Chem. Soc.* **1993**, *115*, 8230.

(11) (a) Ward, M. D. *J. Chem. Soc., Dalton Trans.* **1993**, 1321. (b) Ward, M. D. *J. Chem. Soc., Dalton Trans.* **1994**, 3095.

(12) Downard, A. J.; Honey, G. E.; Phillips, L. F.; Steel, P. J. *Inorg. Chem.* **1991**, *30*, 2259.

(13) Sullivan, B. P.; Salmon, D. J.; Meyer, T. J. *Inorg. Chem.* **1978**, *17*, 3334.

Table 1. Elemental Analyses and Spectroscopic Properties of the New Complexes

complex	anal. (%)[a]			FAB mass spectra[a]		
	C	H	N	m/z	assignment	ν(CO) (cm^{-1})[b]
Re^{I}-AB	44.4 (44.8)	2.1 (2.3)	9.2 (9.1)	617 (616)	$\{(CO)_3ClReL\}$	2023, 1920, 1899
				581 (581)	$\{(CO)_3ReL\}$	
Re^{I}-AB-Re^{I}	34.0 (33.9)	1.7 (1.5)	5.8 (6.1)	922 (922)	$\{[(CO)_3ClRe]_2L\}$	2026, 1924, 1904
				887 (887)	$\{(CO)_3ClReLRe(CO)_3\}$	
Ru^{II}-AB-Re^{I}	39.1 (39.1)	2.3 (2.3)	8.5 (8.5)	1175 (1175)	$\{(bpy)_2RuLRe(CO)_3Cl(PF_6)\}$	2024, 1922, 1901
				1030 (1030)	$\{(bpy)_2RuLRe(CO)_3Cl\}$	
Re^{I}-AB-Ru^{II}	39.6 (39.1)	2.6 (2.3)	8.8 (8.5)	1175 (1175)	$\{(CO)_3ClReLRu(bpy)_2(PF_6)\}$	2025, 1926, 1894
				1030 (1030)	$\{(CO)_3ClReLRu(bpy)_2\}$	

[a] Expected values in parentheses. **Ru^{II}-AB** and **Ru^{II}-AB-Ru^{II}** have been reported previously.[11] [b] Recorded in CH_2Cl_2 solution.

Table 2. Crystallographic Data for $[Cl(CO)_3ReLRu(bipy)_2][PF_6]_2 \cdot 2MeCN \cdot 0.5Et_2O$

Formula: $C_{49}H_{41}ClF_{12}N_{10}O_{3.5}P_2ReRu$	fw: 1438.58
a = 10.449(7) Å	crystal system: triclinic
b = 12.493(8) Å	space group: $P\bar{1}$ (No. 2)
c = 22.906(11) Å	T = 20 °C
α = 92.83(5)°	λ = 0.710 73 Å
β = 101.11(5)°	ϱ_{calc} = 1.738 g cm^{-3}
γ = 109.30(5)°	μ = 2.675 mm^{-1}
V = 2749(3) $Å^3$	wR_2 = 0.128[a] (R_1 = 0.046)[b]
Z = 2	

[a] $wR_2 = [\sum[w(F_o^2 - F_c^2)^2]/\sum w(F_o^2)^2]^{1/2}$ where $w^{-1} = [\sigma^2(F_o^2) + (aP)^2 + bP]$ (a = 0.0679; b = 6.2513) and $P = [\max(F_o^2,0) + 2F_c^2]/3$. The structure was refined on F_o^2 using all data; the value in parentheses is given for comparison with older refinements based on F_o with a typical threshold of $F \geq 4\sigma(F)$ and $R_1 = \sum||F_o| - |F_c||/\sum|F_o|$.

the last by an empirical method based on azimuthal scan data.[14] No correction was made for extinction. Scattering factors are included in SHELX-93.[14] Systematic monitoring of three check reflections at regular intervals showed no significant crystal decay. The structure was solved by direct methods, and successive difference Fourier syntheses were used to locate all non-hydrogen atoms. Initial calculations were performed on a DEC micro-Vax II computer with the SHELXTL PLUS system of programs. All non-hydrogen atoms were refined anisotropically; hydrogen atoms were included in calculated positions and refined isotropically. The final least-squares refinements (on all F^2 data) were carried out on a Silicon Graphics Indigo R4000 computer using SHELXL-93.[14] Refinement converged at wR_2 = 0.129. For comparison with older refinements against F, R_1 = 0.046 using only data with $F > 4\sigma(F)$. The final atomic coordinates are given in Table 3, and selected bond lengths and angles, in Table 4.

Equipment and Methods. ^1H NMR spectra were recorded on JEOL GX270 and GX400 spectrometers. Electron-impact (EI) and fast-atom-bombardment (FAB) mass spectra were measured on a VG-Autospec, in the latter case with 3-nitrobenzyl alcohol as matrix. Cyclic and square-wave voltammograms were obtained using an EG&G PAR model 273A potentiostat controlled by the 270 Research Electrochemistry software. A standard three-electrode configuration was used, with platinum-bead working and auxiliary electrodes and a saturated calomel electrode (SCE) reference. The scan rate was 0.2 V s^{-1}. Ferrocene was added at the end of each experiment as an internal standard; all potentials are quoted *vs* the ferrocene/ferrocenium couple (Fc/Fc^+). The solvent was distilled CH_3CN, containing 0.1−0.2 mol dm^{-3} $[NBu_4][PF_6]$ as base electrolyte.

Ground state absorption spectra were obtained in acetonitrile or DMF/CH_2Cl_2 (9:1, v/v) solutions on a Perkin-Elmer Lambda 2 or Lambda 9 spectrophotometer. The latter solvent was chosen to avoid solubility problems with the Re-containing complexes. Luminescence experiments were performed in DMF/CH_2Cl_2 (9:1, v/v) both at room temperature and at 77 K. Uncorrected luminescence spectra were obtained with a Spex Fluorolog II spectrofluorimeter, and uncorrected band maxima are used throughout. Correction of the luminescence intensity profile was performed either by using software provided by the firm or by employing a calibrated 45-W quartz−halogen tungsten filament lamp by Optronic Laboratories as a standard for the correction of the phototube response. Luminescence quantum yields Φ_s were evaluated by comparing areas under the corrected luminescence spectra on an energy scale and by using the following equation:

$$\frac{\Phi_s}{\Phi_r} = \frac{A_r n_s^2 (\text{area})_s}{A_s n_r^2 (\text{area})_r} \quad (1)$$

where A is the absorbance, n is refractive index of the solvent employed, and s and r stand for sample and reference, respectively. The reference compound was $[Ru(bpy)_3]Cl_2$ in air-equilibrated water (Φ = 0.028).[15] Absorbance values were ≤0.1 at the excitation wavelength. For the DMF/CH_2Cl_2 solvent, n was taken as a compositional average. Luminescence lifetimes were obtained with an IBH single-photon-counting apparatus whose operating lamp employed nitrogen or deuterium. Selection of excitation and emission wavelengths was performed with monochromators or optical filters. The experimental uncertainty in the band maximum for absorption and luminescence spectra is 2 nm; that for luminescence intensity is 20%. The time resolution of the single-photon spectrometer is 200 ps, and the uncertainty on the evaluated lifetimes is 8%.

Results and Discussion

Syntheses of Ligand and Complexes. The bridging ligand L was prepared as described earlier by reaction of 2,2′-bipyridine with $Li[^iPr_2N]$, which results in coupling of the initially-generated bpy radical anions.[11a] The resulting nonsymmetric quaterpyridine was initially thought to be 2,2′:4′,2″:6″,2‴-quaterpyridine—from a C^6/C^4 coupling of the two bpy radical anions—on the basis of the ^1H NMR spectrum (14 inequivalent protons) and the tendency of pyridine[16] and other bipyridines[17] to couple solely at the C^6 and C^4 positions under the same conditions. As not all of the signals are individually resolved, the ^1H NMR spectrum is ambiguous and is apparently consistent with formation of 2,2′:4′,2″:6″,2‴-quaterpyridine.[11a] However the crystal structure of **Re^{I}-AB-Ru^{II}** (see below) showed that L is in fact 2,2′:3′,2″:6″,2‴-quaterpyridine, arising from coupling of two bpy radical anions *via* the C^6 of one bpy and C^3 of the other. Knowing the structure of L, we can now correctly assign the ^1H NMR spectrum (Figure 1). The sets of three protons belonging to the two inner pyridyl rings are marked on the COSY spectrum by solid and dashed lines. $H^{6'}$, $H^{5'}$, and $H^{4'}$ give the signals at 8.80 ppm (dd), 7.49 ppm (dd) ,and 8.15 ppm (dd), respectively (dotted line in Figure 1), and $H^{3''}$, $H^{4''}$, and $H^{5''}$ give the signals at 8.28 ppm (dd), 7.23 ppm (obscured under multiplet), and 7.73 ppm (obscured under

(14) SHELXTL PLUS program system (S320), Nicolet Instrument Corp., 1987; SHELlX93 program system, Siemens Analytical X-ray Instruments, 1989.

(15) Nakamaru, K. *Bull. Chem. Soc. Jpn.* **1982**, *55*, 2697.

(16) (a) Newkome, G. R.; Hager, D. C. *J. Org. Chem.* **1982**, *47*, 599. (b) Hunig, S.; Wehner, I. *Synthesis* **1989**, 552.

(17) (a) Kaufmann, T.; Otter, R. *Chem. Ber.* **1983**, *116*, 479. (b) Hayes, M. A.; Meckel, C.; Schatz, E.; Ward, M. D. *J. Chem. Soc., Dalton Trans.* **1992**, 703.

Table 3. Atomic Coordinates ($\times 10^4$) and Equivalent Isotropic Displacement Parameters ($Å^2 \times 10^3$) for $[(CO)_3ClReLRu(bpy)_2][PF_6]_2 \cdot 2MeCN \cdot 0.5Et_2O$

	x	y	z	$U(eq)^a$		x	y	z	$U(eq)^a$
Re	3964(1)	1991(1)	695(1)	50(1)	C(62)	5181(8)	−1707(6)	4229(3)	55(2)
Ru	3548(1)	−1720(1)	3040(1)	43(1)	C(63)	6244(9)	−1783(8)	4677(3)	70(2)
Cl	2302(3)	2288(3)	1260(1)	103(1)	C(64)	7366(9)	−1964(8)	4535(4)	73(2)
C(1)	5120(9)	3563(7)	853(4)	65(2)	C(65)	7438(8)	−2065(7)	3949(4)	66(2)
O(1)	5791(8)	4516(6)	943(3)	99(2)	C(66)	6376(7)	−1974(6)	3518(3)	54(2)
C(2)	3061(9)	2378(7)	−26(4)	66(2)	N(71)	1834(6)	−1516(5)	2503(2)	49(1)
O(2)	2519(7)	2585(6)	−474(3)	89(2)	C(72)	663(8)	−2370(7)	2213(3)	61(2)
C(3)	5252(8)	1687(9)	266(3)	75(3)	C(73)	−449(9)	−2178(9)	1871(4)	77(2)
O(3)	5938(9)	1536(7)	62(4)	116(3)	C(74)	−369(9)	−1072(9)	1796(4)	77(2)
N(11)	2746(6)	182(5)	607(2)	51(1)	C(75)	820(9)	−193(8)	2079(4)	68(2)
C(12)	3097(7)	−437(6)	1035(3)	47(2)	C(76)	1914(7)	−416(6)	2442(3)	51(2)
C(13)	2272(8)	−1564(6)	1029(3)	56(2)	N(81)	4122(6)	45(5)	3101(2)	48(1)
C(14)	1104(8)	−2056(7)	580(4)	65(2)	C(82)	3172(7)	455(6)	2791(3)	49(2)
C(15)	778(8)	−1443(7)	138(4)	66(2)	C(83)	3400(9)	1605(7)	2833(4)	66(2)
C(16)	1629(8)	−333(7)	161(3)	59(2)	C(84)	4581(10)	2369(7)	3209(4)	72(2)
N(21)	4863(6)	1338(5)	1476(2)	48(1)	C(85)	5517(9)	1940(6)	3534(3)	65(2)
C(22)	5961(8)	2005(7)	1894(3)	58(2)	C(86)	5265(8)	794(6)	3471(3)	55(2)
C(23)	6678(8)	1578(6)	2328(3)	59(2)	P(1)	−50(2)	1245(2)	3697(1)	65(1)
C(24)	6265(8)	405(6)	2331(3)	56(2)	F(1)	1494(8)	1324(11)	3791(4)	194(5)
C(25)	5111(7)	−309(6)	1918(3)	47(2)	F(2)	−1610(6)	1039(9)	3605(3)	151(3)
C(26)	4383(7)	185(6)	1496(3)	45(2)	F(3)	−95(6)	759(6)	4325(2)	99(2)
N(31)	4231(5)	−2193(5)	2279(2)	45(1)	F(4)	429(14)	2438(6)	4011(4)	203(5)
C(32)	4047(7)	−3341(6)	2215(3)	51(2)	F(5)	−449(12)	7(6)	3379(3)	167(4)
C(33)	4586(9)	−3799(7)	1802(4)	68(2)	F(6)	−36(8)	1689(6)	3064(3)	120(2)
C(34)	5256(9)	−3134(7)	1416(4)	71(2)	P(2)	7588(3)	5268(2)	2857(1)	79(1)
C(35)	5378(8)	−1997(7)	1458(3)	59(2)	F(7)	7360(8)	6382(5)	2631(4)	125(2)
C(36)	4847(7)	−1558(6)	1885(3)	47(2)	F(8)	8407(9)	5204(7)	2373(4)	151(3)
N(41)	2797(6)	−3473(5)	2991(2)	51(1)	F(9)	7780(8)	4172(6)	3086(4)	144(3)
C(42)	1976(8)	−4080(7)	3326(4)	65(2)	F(10)	6719(8)	5336(7)	3333(4)	138(3)
C(43)	1617(10)	−5237(7)	3313(5)	82(3)	F(11)	6163(7)	4482(5)	2409(3)	118(2)
C(44)	2126(12)	−5806(8)	2940(5)	96(3)	F(12)	8959(7)	6057(6)	3295(4)	138(3)
C(45)	2948(10)	−5209(7)	2579(5)	80(3)	N(100)	8061(19)	810(18)	1208(7)	202(8)
C(46)	3273(8)	−4043(6)	2608(3)	54(2)	C(101)	8613(42)	1790(19)	1358(19)	297(19)
N(51)	2995(6)	−1505(5)	3837(2)	50(1)	C(102)	9206(23)	3105(19)	1469(13)	276(14)
C(52)	1822(8)	−1327(7)	3900(3)	60(2)	N(200)	1293(32)	−4758(39)	5081(21)	451(23)
C(53)	1514(9)	−1190(8)	4451(4)	69(2)	C(201)	2455(36)	−4665(70)	5116(44)	607(49)
C(54)	2435(10)	−1237(9)	4949(4)	80(3)	C(202)	3890(31)	−4687(32)	5044(20)	412(23)
C(55)	3647(10)	−1400(9)	4895(4)	79(3)	O(301)	0	−5000	0	286(12)
C(56)	3921(8)	−1535(6)	4333(3)	54(2)	C(302)	−1053(20)	−5002(26)	−575(7)	281(14)
N(61)	5254(6)	−1802(5)	3643(2)	47(1)	C(303)	−2238(19)	−5170(17)	−250(10)	202(10)

[a] Defined as one-third of the trace of the orthogonalized U_{ij} tensor.

Table 4. Selected Bond Lengths (Å) and Angles (deg) for $[(CO)_3ClReLRu(bpy)_2][PF_6]_2 \cdot 2MeCN \cdot 0.5Et_2O$

Re−C(1)	1.908(9)	Ru−N(31)	2.135(6)
Re−C(2)	1.905(9)	Ru−N(41)	2.057(6)
Re−C(3)	1.931(7)	Ru−N(51)	2.049(6)
Re−N(11)	2.174(6)	Ru−N(61)	2.069(6)
Re−N(21)	2.180(6)	Ru−N(71)	2.066(6)
Re−Cl	2.464(3)	Ru−N(81)	2.075(6)
C(1)−O(1)	1.148(10)		
C(2)−O(2)	1.158(10)		
C(2)−Re−C(1)	86.3(4)	N(51)−Ru−N(41)	93.1(2)
C(2)−Re−C(3)	88.8(4)	N(51)−Ru−N(71)	96.1(2)
C(1)−Re−C(3)	89.4(4)	N(41)−Ru−N(71)	98.1(2)
C(2)−Re−N(11)	99.5(3)	N(51)−Ru−N(61)	79.1(2)
C(1)−Re−N(11)	174.1(3)	N(41)−Ru−N(61)	85.5(2)
C(3)−Re−N(11)	91.5(3)	N(71)−Ru−N(61)	174.2(2)
C(2)−Re−N(21)	173.2(3)	N(51)−Ru−N(81)	83.6(2)
C(1)−Re−N(21)	100.3(3)	N(41)−Ru−N(81)	174.6(2)
C(3)−Re−N(21)	89.9(3)	N(71)−Ru−N(81)	78.0(2)
N(11)−Re−N(21)	73.9(2)	N(61)−Ru−N(81)	98.1(2)
C(2)−Re−Cl	93.0(2)	N(51)−Ru−N(31)	169.4(2)
C(1)−Re−Cl	92.8(3)	N(41)−Ru−N(31)	78.8(2)
C(3)−Re−Cl	177.2(3)	N(71)−Ru−N(31)	91.8(2)
N(11)−Re−Cl	86.1(2)	N(61)−Ru−N(31)	93.4(2)
N(21)−Re−Cl	88.1(2)	N(81)−Ru−N(31)	105.0(2)

multiplet), respectively (solid line in Figure 1). The two sets of four coupled protons corresponding to the terminal pyridyl rings are also clearly apparent. The C^6/C^3 coupling of the bpy radical anions is surprising, and we do not yet know why it occurs; it is the more remarkable in that L is the *only* significant reaction product.

Syntheses of the mononuclear complexes **Ru^{II}-AB** and **Re^{I}-AB** and of the dinuclear complexes **Ru^{II}-AB-Ru^{II}** and **Re^{I}-AB-Re^{I}** were readily achieved by control of the metal:ligand ratio (slight excess of ligand for mononuclear complexes; >2 equiv of metal for dinuclear complexes). In **Ru^{II}-AB** and **Re^{I}-AB**, we assume that only the less hindered "external" binding site of the ligand is occupied: the product isolated in each case was shown by ^1H NMR spectroscopy to be a single isomer and not a mixture of positional isomers, and although we have no direct structural evidence, it seems reasonable to assume that the less hindered "external" site has been preferentially occupied in each case. Electrochemical and spectroscopic data *(vide infra)* for our mononuclear and dinuclear complexes are consistent with this assumption. The mixed-metal complex **Ru^{II}-AB-Re^{I}** was prepared by reaction of **Ru^{II}-AB** with $[Re(CO)_5Cl]$, and the positional isomer **Re^{I}-AB-Ru^{II}** was likewise prepared from **Re^{I}-AB** and $[Ru(bpy)_2Cl_2] \cdot 2H_2O$. **$Ru^{II}$-AB** and **$Ru^{II}$-AB-$Ru^{II}$** were reported before;[11a] analytical and FAB mass spectroscopic data for the other four complexes are given in Table 1. The FAB mass spectra all show peaks corresponding to the expected mononuclear or dinuclear complex molecules, associated with varying numbers of $[PF_6]^-$ anions in the case of the cationic complexes. All FAB peak clusters have the expected isotopic patterns. ^1H NMR spectra of the dinuclear complexes are

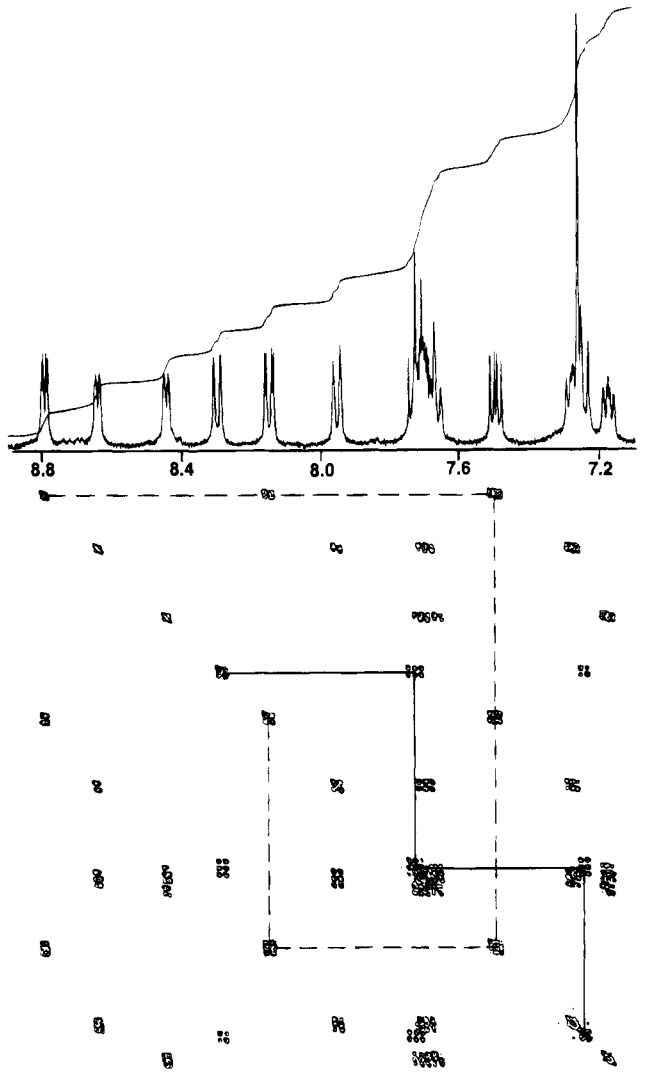

Figure 1. $^1H-^1H$ COSY spectrum ($CDCl_3$, 400 MHz) of L.

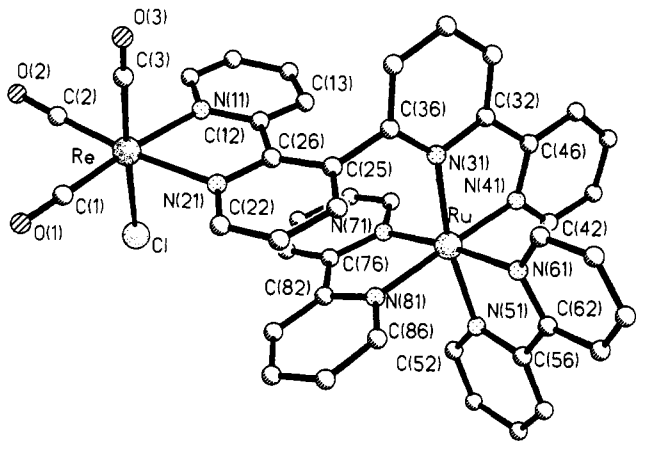

Figure 2. Crystal structure of the cation of $[(CO)_3ClReLRu(bpy)_2][PF_6]_2 \cdot 2MeCN \cdot 0.5Et_2O$.

unhelpful due to the presence of numerous overlapping signals in the aromatic region.

Crystal Structure of Re^I-AB-Ru^{II}. The crystal structure of the cationic part of this complex is shown in Figure 2 (see Tables 2–4). The presence of a 3-substituent on the bpy of the external binding site (**A**) results in a modest dihedral twist of 13.5° between the two pyridyl rings attached to the rhenium atom, but the generally unhindered nature of this binding site is demonstrated by the fact that the Re–N bond lengths are typical of those of other $[Re(bpy)(CO)_3X]$ complexes.[18] In contrast, the $\{Ru(bpy)_2\}^{2+}$ fragment at the internal binding site is in a more sterically hindered environment, as evidenced by the long Ru–N(31) bond [2.135(6) Å] adjacent to the bulky substituent. The Ru–N bonds in $[Ru(bpy)_3]^{2+}$ are all 2.056 Å,[19] and the other five Ru–N bonds of **Re^I-AB-Ru^{II}** are all close to this value. There is a substantial dihedral twist (86°) between the two **A** and **B** bipyridyl fragments of L. As well as being obviously necessary on steric grounds, it results in an aromatic stacking interaction between one of the pyridyl rings at the external site of L and one of the bpy ligands coordinated to the ruthenium(II) center with inter-ring contacts in the typical range of 3.5–4 Å. The Re–Ru separation is 7.251 Å. Various derivatives of $[Ru(bpy)_3]^{2+}$ with sterically hindering derivatives at the bipy-C^6 position have been prepared to study the effects of the distorted coordination environment on their photophysical properties.[20] Only one of these has been crystallographically characterized to our knowledge: $[Ru(bipy)_2(terpy\text{-}N,N')][PF_6]_2$, in which terpy is acting as a bidentate bpy-type ligand with a pendant pyridyl ring at C^6.[20c] This complex is therefore a good structural model for the Ru(II) center of **Re^I-AB-Ru^{II}**, and indeed the bond lengths have a similar spread of values (2.052–2.133 Å) with the longest bond adjacent to the bulky C^6 substitutent.

Electrochemistry. The electrochemical behavior of the complexes is summarized in Table 5. The behavior of **Ru^{II}-AB** and **Ru^{II}-AB-Ru^{II}** has been discussed previously.[11] Briefly, for the dinuclear complex (i) the first reduction is 200 mV easier than that for the mononuclear complex and involves the bridging ligand, (ii) the first metal-centered oxidation is 90 mV more difficult than that for the mononuclear complex, which is due to the higher charge on the complex (+4 rather than +2), and (iii) the two Ru(II)/Ru(III) couples are separated by 70 mV. These results are ascribed to the influence of the second center and indicate that the metal–metal interaction is not negligible.

The Re(I)/Re(II) couple of **Re^I-AB** is, not surprisingly, at a potential similar to that of $[Re(bpy)(CO)_3Cl]$.[9] The first Re(I)/Re(II) couple of **Re^I-AB-Re^I** is at the same potential as that of the mononuclear complex: since **Re^I-AB-Re^I** is neutral, there is no increased charge to destabilize the oxidized species as happens in **Ru^{II}-AB-Ru^{II}** (above). The second oxidation potential of **Re^I-AB-Re^I** is 120 mV more positive than the first, which may be due to a combination of electrostatic interaction between the metals and inequivalence of the metal sites *(vide infra)*. **Re^I-AB** and **Re^I-AB-Re^I** undergo one and two (irreversible) reductions, based on the polypyridyl bridging ligand.[9] The first reduction of **Re^I-AB-Re^I** is 90 mV easier than that for the mononuclear complex, indicating that coordination of the second metal center lowers the level of the π^* orbital of the bridging ligand.

An indication of the inequivalence of the binding sites may be gleaned from comparison of the metal-centered redox potentials of the positional isomers **Ru^{II}-AB-Re^I** and **Re^I-AB-Ru^{II}** (Figure 3). For **Ru^{II}-AB-Re^I** there are clearly identifiable Ru(II)/Ru(III) and Re(I)/Re(II) couples at +0.93 and +1.17 V

(18) (a) Calabrese, J. C.; Tam, W. *Chem. Phys. Lett.* **1987**, *133*, 244. (b) Horn, E.; Snow, M. R. *Aust. J. Chem.* **1980**, *33*, 2369. (c) Guilhem, J.; Pascard, C.; Lehn, J.-M.; Ziessel, R. *J. Chem. Soc., Dalton Trans.* **1989**, 1449.

(19) Rillema, P. D.; Jones, D. S.; Levy, H. A. *J. Chem. Soc., Chem. Commun.* **1979**, 849.

(20) (a) Fabian, R. H.; Klassen, D. M.; Sonntag, R. W. *Inorg. Chem.* **1980**, *19*, 1977. (b) Kelly, J. M.; Long, C.; O'Connell, C. M.; Vos, J. G.; Tinnemans, A. H. A. *Inorg. Chem.* **1983**, *22*, 2818. (c) Constable, E. C.; Hannon, M. J.; Cargill Thompson, A. M. W.; Tocher, D. A.; Walker, J. V. *Supramol. Chem.* **1993**, *2*, 243.

Table 5. Electrochemical Data[a]

complex	metal-based couples		ligand-based couples		
	Ru(II)/Ru(III)	Re(I)/Re(II)[b]			
Ru^{II}-AB[c]	+0.90 (70)		−1.66 (60)	−1.89 (80)	−2.12 (70)
Ru^{II}-AB-Ru^{II}[c]	+0.99, +1.06[d]		−1.46 (60)	−1.73 (60)	−1.86 (70)
Re^{I}-AB		+0.98	−1.68[e]		
Re^{I}-AB-Re^{I}		+0.98, +1.10	−1.55[e]	−1.66	
Ru^{II}-AB-Re^{I}	+0.93 (80)	+1.17	−1.56[e]	−1.77	−1.99
Re^{I}-AB-Ru^{II}	+1.04[f]		−1.49[e]	−1.77	−1.98

[a] Potentials are in V *vs* Fc/Fc^+; solvent was CH_3CN; cyclic voltammetric peak−peak separations ΔE_p for chemically reversible processes are in parentheses where available. [b] Irreversible processes; peak potentials taken from square-wave voltammograms. [c] From ref 11. [d] Two (assumed reversible) metal-based oxidations not separable by cyclic voltammetry; peak potentials are taken from the square-wave voltammogram. [e] Poorly resolved, irreversible sequence of ligand-based reductions; the quoted peak potentials are taken from square-wave voltammograms. [f] Re-based and Ru-based redox couples occur at very similar potentials and are not resolvable; the peak potential quoted is from the square-wave voltammogram.

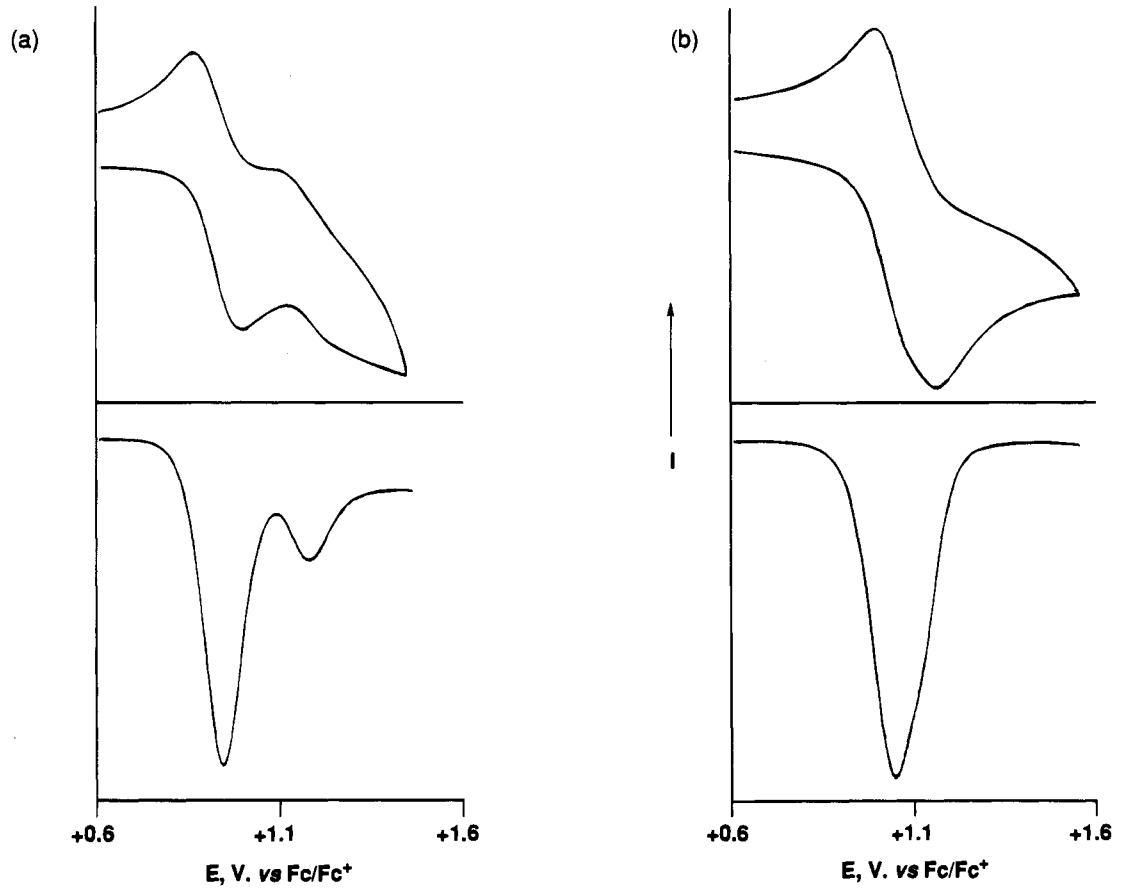

Figure 3. Cyclic and square-wave voltammograms of (a) **Ru^{II}-AB-Re^{I}** and (b) **Re^{I}-AB-Ru^{II}** in MeCN. Potentials are *vs* Fc/Fc^+; the *y* axis is current (arbitrary units).

vs Fc/Fc^+, respectively (Figure 3a);[21] the Ru(II)/Ru(III) couple is fully reversible but for the Re(I)/Re(II) couple the return wave is less intense than the outward wave, which is typical behavior.[9a] For **Re^{I}-AB-Ru^{II}** in contrast the two metal-centered redox potentials are sufficiently close together not to be resolvable, a single combined wave occurring at +1.04 V *vs* Fc/Fc^+, (Figure 3 b). The oxidation potentials of both types of metal center in these complexes are therefore made *ca.* 100 mV more positive on moving from the external (**A**) site to the internal (**B**) site. There will be steric and electronic contributions to this which cannot easily be separated. The steric inequivalence of the sites arises from the more hindered coordination environment at the inner site, as shown in the crystal structure of **Re^{I}-AB-Ru^{II}**; the electronic inequivalence arises from the fact that the external bpy binding site is substituted at the C^3 position whereas the internal binding site is substituted at the C^6 position (Chart 1). Three observations suggest that it is the electronic effects that dominate. First, the Ru(II)/Ru(III) redox couple of the sterically hindered complex $[Ru(bpy)_2(tolbpy)]^{2+}$ (tolbpy = 6-*p*-tolyl-2,2′-bipyridine) is not very different from that of $[Ru(bpy)_3]^{2+}$.[20b] Second, it is known that altering the position of substituents on bpy ligands can have a strong effect on metal-based redox potentials.[6,22] Third, the difference between the redox potentials of $[Ru(bpy)_3]^{2+}$ fragments in the two binding sites of **Ru^{II}-AB-Ru^{II}** is only 70 mV, some of which may be ascribed to electrostatic interaction between the metal centers, so the contribution to this arising from the different coordination environments of the two metal

(21) The Fc/Fc^+ couple is +0.38 V *vs* SCE in acetonitrile.

(22) (a) Skarda, V.; Cook, M. J.; Lewis, A. P.; McAuliffe, G. S. G.; Thomson, A. J.; Robbins, D. J. *J. Chem. Soc., Perkin Trans. 2* **1984**, 1309. (b) DeLaive, P. J.; Foreman, T. K.; Graetzel, M.; Whitten, D. G. *J. Am. Chem. Soc.* **1980**, *102*, 5627.

Table 6. Absorption Maxima[a]

complex	λ_{max} (nm) ($10^{-3}\epsilon$ (dm^3 mol^{-1} cm^{-1}))			
Ru^{II}-AB	457 (14)	425 (sh)		287 (97)
Ru^{II}-AB-Ru^{II}	452 (23)	427 (sh)		288 (121)
Re^{I}-AB	378 (3.8)		320 (sh)	294 (16)
Re^{I}-AB-Re^{I}	385 (8)		330 (sh)	316 (23)
Ru^{II}-AB-Re^{I}	456 (14)	425 (sh)	330 (sh)	289 (76)
Re^{I}-AB-Ru^{II}	453 (13)	423 (sh)		289 (86)

[a] In DMF/CH_2Cl_2 solvent (9:1, v/v).

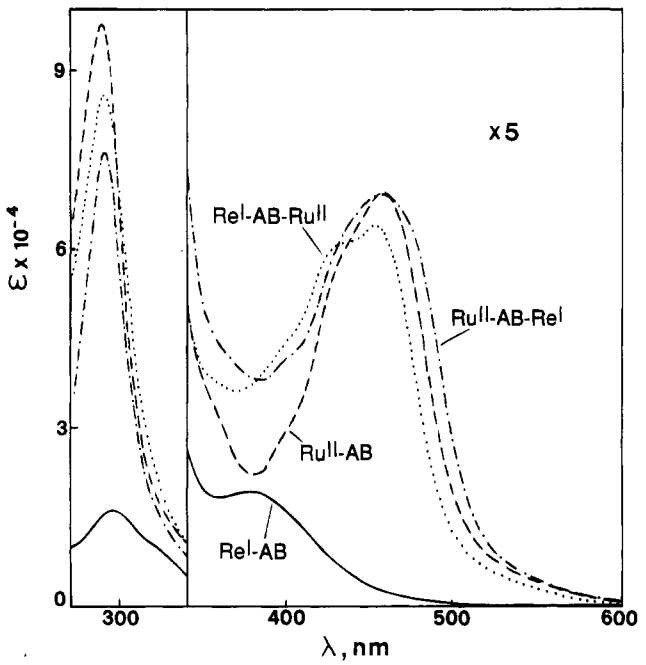

Figure 4. Absorption spectra of **Re^{I}-AB** (—), **Ru^{II}-AB** (– –), **Re^{I}-AB-Ru^{II}** (· · ·), and **Ru^{II}-AB-Re^{I}** (– · –).

centers must be correspondingly small. If we consider the complexes **Ru^{II}-AB-Re^{I}** and **Re^{I}-AB-Ru^{II}** as $[Ru(bpy)_3]^{2+}$ derivatives with an electron-withdrawing $[Re(bpy)(CO)_3Cl]$ substituent attached to C^3 in the former case and to C^6 in the latter, it is apparent that the substituent effect is greater in the latter case as the shifts in the Ru(II)/Ru(III) couples are +30 mV and *ca.* +140 mV, respectively, compared to **Ru^{II}-AB**. Likewise the effect of the electron-withdrawing $[Ru(bpy)_3]^{2+}$ substituent on the redox potentials of the $[Re(bipy)(CO)_3Cl]$ is to shift it by +190 mV when attached at a C^6 position in **Ru^{II}-AB-Re^{I}** and *ca.* +60 mV when attached at a C^3 position in **Re^{I}-AB-Ru^{II}**.

Absorption Spectra. Ground state absorption properties are summarized in Table 6 and the spectra for the mononuclear and the heterodinuclear complexes are illustrated in Figure 4. All the complexes exhibit intense absorptions in the 290−320 nm interval, which are characteristics of ligand-centered (LC) transitions.[6,8−10] The spectra of the complexes containing the Ru-based chromophore show a band maximum between 452 and 457 nm, which corresponds to a ^{1}MLCT transition. When a single Ru center is present, the ^{1}MLCT band exhibits an extinction coefficient, ϵ, of *ca.* 14 000 dm^3 mol^{-1} cm^{-1} (Figure 4). In **Ru^{II}-AB-Ru^{II}** the value of ϵ is higher but not double. On passing from **Ru^{II}-AB** to **Ru^{II}-AB-Ru^{II}**, the MLCT band maximum moves to a slightly higher energy, from 457 to 452 nm, respectively. This result seems inconsistent with the known linear relationship between electrochemistry and spectroscopy for compounds forming MLCT excited states.[6,8−10] Actually, from the electrochemical results seen above one would have expected a lower energy for the MLCT maximum in the dinuclear complex than in the mononuclear one. A possible explanation for the spectroscopic behavior could be based on the fact that there are two types of Ru → L CT transitions, one involving the terminal bpy ligands and the other invoving the bridging ligand L. According to the electrochemical results, the Ru → L transition should occur at lower energy in **Ru^{II}-AB-Ru^{II}** than in **Ru^{II}-AB**; however, its intensity is expected to be lower than that associated with the Ru → bpy transition for statistical reasons. Thus it seems likely that the overall (slight) hypsochromic shift of the MLCT absorption maximum is due to a splitting of the closely-spaced Ru → L and Ru → bpy components, resulting in a larger width of the absorption profile.[11a]

Table 7. Luminescence Properties[a]

	298 K					77 K	
complex	λ_{max} (nm)	τ (ns)	Φ	$10^{-4}k_r$ (s^{-1})	$10^{-6}k_{nr}$ (s^{-1})	λ_{max} (nm)	τ (μs)
Ru^{II}-AB	633	250	1.9×10^{-2}	7.6	3.9	595	5.4
Ru^{II}-AB-Ru^{II}	656	340	2.2×10^{-2}	6.5	2.9	615	5.3
Re^{I}-AB	626	11	9.2×10^{-4}	8.4	91.0	535	3.2
Re^{I}-AB-Re^{II}	622	9	5.3×10^{-4}	5.9	110.0	548	2.7
Ru^{II}-AB-Re^{I}	644	410	2.8×10^{-2} [b]	6.8	2.4	607	4.7
Re^{I}-AB-Ru^{II}	623	23	1.4×10^{-3} [c]	6.1	43.0	590	5.8

[a] In aerated DMF/CH_2Cl_2 solvent. [b] Excitation performed at 470 nm. [c] Excitation performed at 480 nm.

For **Re^{I}-AB** the lowest energy maximum occurs at 378 nm (Figure 4) and is assigned to a ^{1}MLCT process by comparison with $[Re(bpy)(CO)_3Cl]$, whose lowest energy ^{1}MLCT maximum occurs at at 370 nm.[9a] The small difference in energy between the two may be explained by the more extended aromatic network of L compared to bpy. Coordination of the second metal fragment in **Re^{I}-AB-Re^{I}** lowers the π^* level further such that λ_{max} is centered at 385 nm. This is consistent with the electrochemical results seen above for **Re^{I}-AB** and **Re^{I}-AB-Re^{I}**.

For the heterodinuclear complexes **Ru^{II}-AB-Re^{I}** and **Re^{I}-AB-Ru^{II}**, the ruthenium-based ^{1}MLCT band maxima occur at 456 and 453 nm, respectively (Table 6, Figure 4), and in both cases the band masks the weaker rhenium-based MLCT band, which is expected to lie at a higher energy. The position of λ_{max}(MLCT) for the ruthenium centers in the heterodinuclear complexes should be related to some extent to the inequivalence of the coordinating sites of L; actually we find only a small difference in the ground state Ru → **A** and Ru → **B** absorption maxima (where **A** and **B** are the different bipridyl fragments of L) for the two heterodinuclear complexes. Other workers have reported that distortion of the Ru(II) coordination sphere by introducing bulky substituents at the bipyridine C^6 positions has little effect on the position of λ_{max}(MLCT).[20] These observations should be compared with those on the metal-centered oxidation processes which indicate that the Ru center is easier to oxidize when attached to the **A** than when attached to the **B** site. It appears that the lowest-lying ^{1}MLCT level of the $[Ru(bpy)_2(\mathbf{A})]^{2+}$ fragment lies at a slightly lower energy than the $[Ru(bpy)_2(\mathbf{B})]^{2+}$ fragment. The energy levels for the ^{3}MLCT luminescent states at 77 K provide a stronger evidence for the inequivalence of the binding sites of L (see below).

Luminescence Properties. Emission band maxima and lifetimes at room temperature and at 77 K are collected in Table 7. Representative luminescence spectra are shown in Figure 5. A single emission was observed for all of the dinuclear complexes. The room-temperature luminescence quantum yields are also reported in the table together with the rates for radiative (k_r) and nonradiative (k_{nr}) processes, eq 2, deactivating the luminescent excited state.

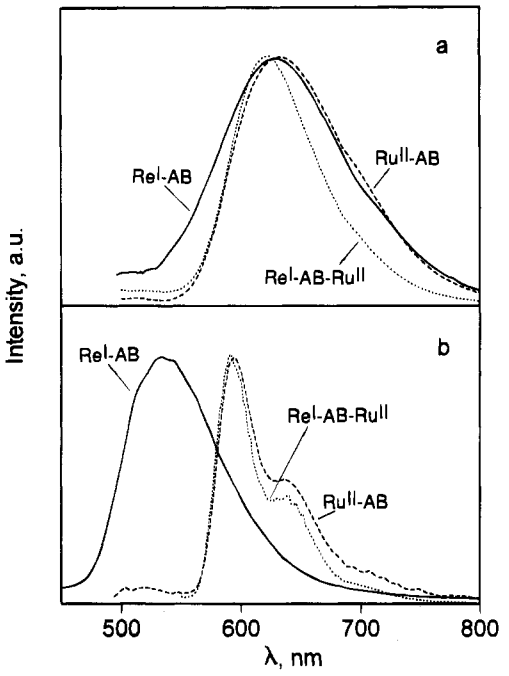

Figure 5. Luminescence spectra of **Re^{I}-AB** (—), **Ru^{II}-AB** (- - -), and **Re^{I}-AB-Ru^{II}** (• • •). Top panel: $T = 298$ K. Bottom panel: $T = 77$ K.

$$k_r = \frac{\Phi}{\tau} \tag{2a}$$

$$k_{nr} = \frac{1}{\tau} - k_r \tag{2b}$$

At 77 K the luminescence spectra for **Ru^{II}-AB**, **Ru^{II}-AB-Ru^{II}**, **Ru^{II}-AB-Re^{I}**, and **Re^{I}-AB-Ru^{II}** show vibrational progressions with spacing of *ca.* 1350 cm^{-1}, as expected for Ru–polypyridine emitters in frozen solvent.[6,23] In contrast, the 77 K luminescence spectra of **Re^{I}-AB** and **Re^{I}-AB-Re^{I}** are broad and structureless, which is typical of MLCT Re-based emitters.[9,10] At room temperature the luminescence spectra of all complexes are structureless.

The mononuclear **Ru^{II}-AB** and **Re^{I}-AB** complexes have their emission maxima at similar positions at room temperature—633 and 626 nm, respectively—whereas at 77 K (in frozen solvent) they are centered at rather different wavelengths, 595 and 535 nm, respectively (Table 7, Figure 5). This behavior can be traced back to (a) the electronic nature of the two chromophores and (b) the role of the solvent. We shall discuss this finding in some detail because it is of relevance to the understanding of the spectroscopic properties for the series of complexes investigated.

(a) For both mononuclear complexes the excited state responsible for the luminescence is of MLCT nature, at both room and low temperature. This assignment is based on the following luminescence properties: (i) at room temperature the luminescence spectra of both complexes are broad and structureless (Figure 5a) and the luminescence lifetimes and quantum yields are similar to those of $[Ru(bpy)_3]^{2+}$ [6] and $[Re(L)(CO)_3Cl]$,[9a,10a] respectively, with L = bpy or related ligands, whose emissions were previously assigned as coming from MLCT states; (ii) at 77 K the luminescence spectrum of **Ru^{II}-AB** is resolved into vibronic bands (Figure 5b), is centered at a slightly shorter wavelength than at room temperature, and exhibits a lifetime again very close to that of the MLCT excited state of $[Ru(bpy)_3]^{2+}$;[6] (iii) at 77 K the luminescence spectrum of **Re^{I}-AB** is broad, strongly shifted to higher energy than at room temperature, and its lifetime is typical of a Re-based MLCT emitter.[8-10]

(b) The **Ru^{II}-AB** and **Re^{I}-AB** chromophores exhibit quite different Stokes shifts, eq 3, amounting to *ca.* 6100 and 10 500 cm^{-1}, respectively.

$$E_{abs} - E_{em} = E_{S-T} + 2\lambda \tag{3}$$

In the above equation E_{abs} and E_{em} are the energies corresponding to the spectroscopic band maxima for absorption and emission, and E_{S-T} is the singlet–triplet energy separation for orbitally equivalent singlet and triplet excited states.[24] λ is a reorganization energy which includes contributions from solvent and intramolecular terms, λ_s and λ_v, respectively. The difference in Stokes shift between **Re^{I}-AB** and **Ru^{II}-AB** is mainly ascribed to the fact that an MLCT transition is accompanied by (i) a polar solvent rearrangement, which will be more substantial for the neutral **Re^{I}-AB** complex than for the **Ru^{II}-AB** dication, and (ii) an intramolecular rearrangement, which will be more important for **Re^{I}-AB** because of the electron-donating ability of the carbonyl groups.[8,9] An assessement of the importance of λ_s may be obtained by noting that, in passing from room temperature to 77 K, the luminescence band maximum (i) for **Re^{I}-AB** moves from 626 to 535 nm, amounting to an energy difference of ~2700 cm^{-1}, and (ii) for **Ru^{II}-AB** moves from 633 to 595 nm, for an energy difference of ~1000 cm^{-1} (Table 7). Thus, $\lambda_s^{Re} > \lambda_s^{Ru}$ and in frozen solvent the MLCT luminescent level of **Re^{I}-AB** is more destabilized than that of **Ru^{II}-AB** because of the lack of solvent repolarization. The spectral properties of the homometallic dinuclear complexes are similarly affected by the state of the solvent. From the luminescence results of Table 7 one sees that, in passing from room temperature to 77 K, the energy differences in band maxima for **Ru^{II}-AB-Ru^{II}** and **Re^{I}-AB-Re^{I}** are ~1000 and ~2200 cm^{-1}, respectively.

It is also useful to compare the luminescence properties of the mononuclear and dinuclear complexes. Thus, comparing **Ru^{II}-AB** and **Ru^{II}-AB-Ru^{II}**, we find that the luminescence band maximum is at lower energy for the dinuclear complex, both at room temperature and at 77 K (Table 7). This behavior is due to the stabilizing effect of the second metal center on the π^* level of the bridging ligand, i.e. the ligand involved in the MLCT transition responsible for the luminescence. The increase in luminescence intensity and lifetime exhibited by the dinuclear species at room temperature may be ascribed to stabilization of the luminescent MLCT level and consequent increased energy gap between this level and higher lying metal-centered (MC) levels responsible for fast radiationless processes.[6] The luminescence and photophysical properties (particularly τ, Φ, and k_{nr}) of **Ru^{II}-AB-Re^{I}** are very close to those of **Ru^{II}-AB** and **Ru^{II}-AB-Ru^{II}** (Table 7) and reveal that for **Ru^{II}-AB-Re^{I}** luminescence is Ru-centered.

For **Re^{I}-AB** and **Re^{I}-AB-Re^{I}** one sees that the band maximum of the dinuclear complex relative to the mononuclear complex is positioned at higher energy at room temperature but at lower energy at 77 K (the luminescent level of the dinuclear complex is *less* stabilized at room temperature but is also *less* destabilized in frozen solvent, with respect to that of the **Re^{I}-AB** complex). This can be understood by considering that the MLCT emission

(23) (a) Caspar, J. V.; Meyer, T. J. *Inorg. Chem.* **1983**, *22*, 2444. (b) Kober, E. M.; Caspar, J. V.; Lumpkin, R. S.; Meyer, T. J. *J. Phys. Chem.* **1986**, *90*, 3722. (c) Barkawi, K. R.; Murtaza, Z.; Meyer, T. J. *J. Phys. Chem.* **1991**, 95, 47.

(24) $E_{S-T} = 2K$, where K (the exchange integral) is related to the overlap between metal- and ligand-centered orbitals. For the electronically similar $[Os(bpy)_3]^{2+}$ species, $E_{S-T} \sim 3600$ cm^{-1}, as estimated from the absorption spectrum.[6]

is centered on the Re moiety attached to **A**, in agreement with the electrochemical behavior, and by realizing that the presence of the second Re center results in $\lambda^{ReRe} < \lambda^{Re}$, consistent with the spectral shifts exhibited by the two complexes in passing from fluid to rigid solvent.

For the heterodinuclear complex **Re^{I}-AB-Ru^{II}** we assign the rhenium center as being responsible for the room-temperature luminescence, on the basis that its luminescence and photophysical properties are very similar to those of **Re^{I}-AB** and **Re^{I}-AB-Re^{I}** (Table 7). In frozen solvent however the Re-based level of **Re^{I}-AB-Ru^{II}** is expected to be more destabilized than the close-lying Ru-based level, since $\lambda_s^{Re} > \lambda_s^{Ru}$. Indeed, from the vibronically resolved luminescence profile, the band maximum, and the lifetime values, it is apparent that at 77 K luminescence changes to Ru-centered in **Re^{I}-AB-Ru^{II}** (Figure 5 and Table 7). At 77 K the Ru-based luminescence bands for **Ru^{II}-AB-Re^{I}** and **Re^{I}-AB-Ru^{II}** are centered at 607 and 590 nm, respectively, which indicates that the inequivalent **A** and **B** sites of L cause a difference in energy between the $[Ru(bpy)_2(\mathbf{A})]^{2+}$ and $[Ru(bpy)_2(\mathbf{B})]^{2+}$ luminescent levels amounting to *ca.* 500 cm^{-1}.

It is worth pointing out that some workers have found that distortion of the ruthenium coordination environment arising from a bulky substitutent at the C^6 position of one of the bipyridine ligands drastically reduces the emission intensity.[20] However this does not seem to be a problem with these complexes, as the above results show that at 77 K emission from the ruthenium fragment at the hindered site **B** of **Re^{I}-AB-Ru^{II}** still occurs. Similar results were found in the related **Ru^{II}-AB-Os^{II}** and **Os^{II}-AB-Ru^{II}** complexes, for which the osmium-based emissions in each case have comparable lifetimes and quantum yields despite the difference in the coordination geometries of the $\{Os(bpy)_3\}^{2+}$ fragments in the different sites.[25]

Intramolecular Energy Transfer in Ru^{II}-AB-Re^{I} and Re^{I}-AB-Ru^{II} Complexes. From the luminescence properties discussed above, we conclude that at room temperature the lowest-lying luminescent level is Ru-centered in **Ru^{II}-AB-Re^{I}** and Re-centered in **Re^{I}-AB-Ru^{II}**. In order to investigate the inter-center photoinduced energy-transfer process in both heterodinuclear complexes, we performed either (i) selective excitation of the Ru-based chromophore in the 470−480 nm interval or (ii) an approximately 1:1 statistical excitation of both the Re- and Ru-based chromophores by using light in the 370−395 nm interval (Figure 4).

For **Ru^{II}-AB-Re^{I}**, with $\lambda_{exc} = 395$ nm, we observed complete Re → Ru energy transfer at room temperature because the obtained luminescence, centered at 644 nm and characterized by $\tau = 400$ ns, exhibited a luminescence quantum yield[26] $\Phi = 2.7 \times 10^{-2}$, i.e. identical to that obtained by selectively exciting the Ru-based chromophore (Table 7). Similarly for **Re^{I}-AB-Ru^{II}**, by employing either 480 or 380 nm light excitation at room temperature, we obtained a Re-based luminescence (Table 7) exhibiting the same quantum yield[26] in both cases, consistent with complete Ru → Re energy transfer. At 77 K the luminescence features of both heterodinuclear complexes under low and high energy excitation were ascribable to the lowest-lying Ru-based chromophore (see above).

In order to discuss the energy transfer between the component chromophores, one takes into account two possible mechanisms: the Förster-type transfer,[27] which occurs via Coulombic interaction between deactivation of the donor and excitation of the acceptor, and the Dexter mechanism[28] which operates through exchange interaction between the involved partners. According to the Förster approach, the energy-transfer rate can be evaluated by using some spectroscopic quantities, as detailed in eq 4, where Φ_D and τ_D are the luminescence quantum yield

$$k_{en}^{F} = 5.87 \times 10^{-25} \frac{\Phi_D}{n^4 \tau_D r^6} \int_0^\infty F_D(\bar{\nu}) \epsilon_A(\bar{\nu})\, d\bar{\nu}/\bar{\nu}^4 \qquad (4)$$

and lifetime of the donor, n is the refractive index of the solvent, and $F_D(\bar{n})$ and $\epsilon_A(\bar{n})$ are the donor luminescence and the acceptor absorption spectra (cm^{-1}).

For practical reasons the spectroscopic parameters of the Ru- and Re-based fragments of the heterodinuclear complexes have been approximated by those of the $[Ru(bpy)_2L]^{2+}$ and $[Re(CO)_3ClL]$ mononuclear species.[29] The metal−metal distance was taken as $r = 7.25$ Å, in agreement with the X-ray results of Figure 2.

For **Ru^{II}-AB-Re^{I}** $\Phi_D = 9.2 \times 10^{-4}$, $\tau_D = 11$ ns, the spectral overlap integral of eq 4 is 7.1×10^{-16} $dm^3\ mol^{-1}\ cm^3$ and $k_{en}^{F} = 6.8 \times 10^7\ s^{-1}$. Since the room temperature photophysical results discussed above indicate that complete quenching (within a few percent uncertainty) of the donor luminescence has occurred, one concludes that the experimental rate of energy transfer is greater than the intrinsic deactivation of the Re-based chromophore, $k_{en}^{exp} > 10^9\ s^{-1}$. This result rules out the Förster mechanism as being responsible for Re → Ru photoinduced energy transfer in **Ru^{II}-AB-Re^{I}**.

For **Re^{I}-AB-Ru^{II}**, the results are even more clear-cut because inspection of Figures 4 and 5 reveals that the spectral overlap of eq 4 for Ru → Re energy transfer is negligible. Thus, also for this dinuclear species, energy transfer takes place via a Dexter exchange-type mechanism.

Conclusion. We have prepared and characterized a series of mono- and dinuclear complexes of the asymmetric bridging ligand L, containing $\{Ru(bpy)_2\}^{2+}$ and/or $\{Re(CO)_3Cl\}$ fragments coordinated to the bipyridyl binding sites. We have found that in the dinuclear **Ru^{II}-AB-Re^{I}** and **Re^{I}-AB-Ru^{II}** species (i) the luminescence is Ru- and Re-based, respectively, and (ii) the photoinduced energy transfer from the higher-lying (Re- and Ru- based, respectively) to the luminescent component chromophores takes place via an exchange mechanism. This result is in agreement with the close separation distance between the metal centers and with the fact that the metal centers are linked by a conjugated bridging ligand.

Acknowledgment. This work was supported by the Progetto Strategico Tecnologie Chimiche Innovative of the National Research Council of Italy and by the EPSRC (U.K.) We thank L. Ventura and M. Minghetti for technical help.

Supplementary Material Available: Tables of X-ray experimental details and crystallographic data, anisotropic thermal parameters, and bond distances and angles for $[(CO)_3ClReLRu(bpy)_2][PF_6]_2 \cdot 2MeCN)_2 \cdot 0.5Et_2O$ (8 pages). Ordering information is given on any current masthead page.

IC9413880

(25) Balzani, V.; Bardwell, D. A.; Barigelletti, F.; Cleary, R. L.; Guardigli, M.; Sovrani, T.; Ward, M. D. Manuscript in preparation.
(26) Φ was determined by comparing the luminescence intensity of the sample with that of $[Ru(bpy)_3]Cl_2$[15] in air-equilibrated water under identical excitation conditions and according to eq 1 of the text.
(27) Förster, Th. H. *Discuss. Faraday. Soc.* **1959**, *27*, 7.
(28) Dexter, D. L. *J. Chem. Phys.* **1953**, *21*, 836.
(29) We have seen above that the spectroscopic properties of the Ru- and Re-based chromophores are somewhat different when they are attached to the **A** or **B** sites of the bridging ligand L. However our approximation seems justified because the photophysical changes for the two chromophores are expected to be relatively small and should not lead to relevant differences in the estimated energy-transfer rates.